Binding of Trastuzumab to ErbB2 Is Inhibited by a High Pericellular Density of Hyaluronan

Tímea Váradi, Tamás Mersich, Päivi Auvinen, Raija Tammi, Markku Tammi, Ferenc Salamon, István Besznyák Jr., Ferenc Jakab, Zsolt Baranyai, János Szöllősi, and Peter Nagy

Department of Biophysics and Cell Biology, Medical and Health Science Centre, University of Debrecen, Debrecen, Hungary (TV,JS,PN); Department of Surgery and Vascular Surgery, Uzsoki Teaching Hospital, Budapest, Hungary (TM,IB,FJ,ZB); Department of Oncology, Kuopio University Hospital, Kuopio, Finland (PA); Institute of Biomedicine, University of Eastern Finland, Kuopio, Finland (RT,MT); Department of Pathology, Uzsoki Teaching Hospital, Budapest, Hungary (FS); and Cell Biology and Signaling Research Group of the Hungarian Academy of Sciences, Medical and Health Science Centre, University of Debrecen, Debrecen, Hungary (JS).

Summary

Although trastuzumab is an efficient drug, primary and acquired resistance is a challenging problem. The authors have previously shown in mouse xenograft experiments that masking ErbB2 by hyaluronan leads to diminished binding of the antibody and consequent resistance. In the current work, they correlated trastuzumab binding with the pericellular density of hyaluronan in ErbB2-overexpressing human breast cancer samples. A method for quantifying the relative binding of trastuzumab was developed involving constant and low-frequency background subtraction, segmenting the image to membrane and background pixels followed by evaluation of trastuzumab fluorescence, normalized with the expression level of ErbB2, only in the membrane. The normalized binding of trastuzumab showed a negative correlation with the pericellular density of hyaluronan ($r = -0.52$) with the effect being the most pronounced in the extreme cases (i.e., low and high hyaluronan densities predicted strong and weak binding of trastuzumab, respectively). Removal of hyaluronan by hyaluronidase digestion unmasked the trastuzumab binding epitope of ErbB2 demonstrated by a significantly increased normalized binding of the antibody. The results show that the accumulation of pericellular hyaluronan plays a crucial role in masking ErbB2. (J Histochem Cytochem 60:567–575, 2012)

Breast cancer is a heterogeneous disease whose genotype varies not only between individual patients but also within a single patient during progression, calling for targeted therapies tailored to the given tumor (Lőrincz et al. 2006; Lower et al. 2009; Di Cosimo and Baselga 2010). Tremendous progress has been made in the design and application of specific inhibitors and monoclonal antibodies against signal transducing proteins whose overexpression in cancer cells implies that they fulfill critical roles in maintaining the malignant phenotype (Weinstein and Joe 2008). Somewhat disappointing is the fact that despite the huge expectations, relatively small improvements have been achieved in survival times due to the development of resistance and the lack of a sufficient understanding of which proteins are to be targeted in specific tumor types (Di Cosimo and Baselga 2010).

Corresponding Author:
Peter Nagy, Department of Biophysics and Cell Biology, Medical and Health Science Centre, University of Debrecen, Nagyerdei krt. 98, 4032 Debrecen, Hungary.
E-mail: nagyp@med.unideb.hu

ErbB proteins are at the forefront of interest in rational drug development. They constitute a family of transmembrane receptor tyrosine kinases taking part in both physiological and pathological signaling processes (Hynes and MacDonald 2009). Overexpression of ErbB2, a family member lacking a soluble ligand, has been strongly linked to poor prognosis in breast cancer (Ross et al. 2003). In addition to serving as a prognostic factor, ErbB2 is targeted by low molecular weight tyrosine kinase inhibitors and monoclonal antibodies (Di Cosimo and Baselga 2008). Trastuzumab, a humanized monoclonal antibody against ErbB2, offers a significant benefit for patients with ErbB2-overexpressing breast cancer in combination with conventional chemotherapy (Smith et al. 2007). Its mechanism of action is thought to involve antibody- or complement-mediated cytotoxicity and direct inhibitory effects on the ErbB2-expressing cells (Clynes et al. 2000; Nahta and Esteva 2006; Barok et al. 2007). The latter includes diminished signaling through ErbB2 and Src and subsequent activation of the phosphatase and tensin homolog (PTEN) phosphatase (Nagata et al. 2004) and disruption of the ErbB2-ErbB3 complex, resulting in inhibition of Akt-mediated signaling (Hynes and MacDonald 2009; Junttila et al. 2009). These primary effects lead to arrest of the cell cycle in the G1 phase (Lane et al. 2001), induction of apoptosis (Nahta and Esteva 2006), inhibition of ErbB2 ectodomain cleavage (Molina et al. 2001), angiogenesis (Izumi et al. 2002), and DNA repair (Nahta and Esteva 2006). The relatively minor side effects of trastuzumab are also thought to be based on the inhibition of ErbB-mediated signaling in the heart (Pentassuglia and Sawyer 2009). The application of trastuzumab in combination with other drugs prevents the accurate assessment of the development of resistance to the antibody itself, but a decline in responsiveness during long-term treatment is very common (Mukohara 2011). A multitude of factors have been implicated in trastuzumab resistance, including loss of PTEN expression (Nagata et al. 2004); activating mutations in the catalytic subunit of PI3K (phosphoinositide 3-kinase) (Junttila et al. 2009); increased signaling through other ErbB proteins, Met or IGF1R (insulin-like growth factor 1 receptor) (Mukohara 2011); overexpression of calpain-1 (Storr et al. 2011); and expression of a constitutively dimerized, truncated form of ErbB2 by alternative initiation of translation (Sperinde et al. 2010). We have shown previously that masking of the trastuzumab binding epitope of ErbB2 by MUC4 or hyaluronan also leads to trastuzumab resistance (Nagy et al. 2005; Pályi-Krekk et al. 2007). In particular, the role of hyaluronan was established by showing that inhibition of its synthesis led to increased binding and antiproliferative effect of trastuzumab in vitro and in mouse xenograft experiments (Pályi-Krekk et al. 2007). However, such correlations have not been confirmed in human tumor samples.

In addition to its aforementioned role, hyaluronan plays other important roles in carcinogenesis (Sironen et al. 2011). In tumors, hyaluronan is produced by hyaluronan synthases (HAS1–3) in the malignant cells themselves or in stromal cells (Toole et al. 2002; Weigel and DeAngelis 2007). Hyaluronan provides a supportive matrix for cellular growth and motility and creates a pericellular zone of exclusion, blocking the access of materials to the cell surface (Rilla et al. 2008). In addition, it also plays a more active role by stimulating proliferation (Udabage et al. 2005; Twarock et al. 2011), migration (Bourguignon et al. 2007; Urakawa et al. 2012), angiogenesis (Takahashi et al. 2005), multidrug resistance (Misra et al. 2005), and epithelial-mesenchymal transition (Toole et al. 2005; reviewed in Sironen et al. 2011). The latter responses are induced by the binding of hyaluronan or its low molecular weight degradation products to cell-surface receptors (CD44, RHAMM) (Day and Prestwich 2002). These receptors either directly stimulate cellular responses or are integrated into a multiprotein signaling platform involving ErbB proteins (Pályi-Krekk et al. 2008; Sironen et al. 2011). Hyaluronan seems to play a double-faceted role in malignancy. Adenocarcinomas with high hyaluronan content tend to grow aggressively and are poorly differentiated, whereas, in squamous cell carcinomas, reduced hyaluronan content is associated with higher malignancy (Sironen et al. 2011). In particular, overproduction of hyaluronan in mammary carcinoma accelerates tumor growth through the recruitment of stromal cells, which stimulates angiogenesis, and is associated with poor prognosis (Auvinen et al. 2000; Wernicke et al. 2003; Itano and Kimata 2008).

Although the role of hyaluronan has been thoroughly investigated in human tumors, we have undertaken this study to establish if it is involved in inhibiting trastuzumab binding to ErbB2 in human breast cancer in vivo as expected based on our previous in vitro and xenograft experiments (Pályi-Krekk et al. 2007). In the current article, we show that pericellular hyaluronan density is inversely correlated with trastuzumab binding and suggest that this effect may contribute to the negative prognostic value of hyaluronan overproduction in breast cancer.

Materials and Methods

Patients and Tissue Samples

Patients diagnosed with ErbB2-overexpressing breast cancer at the Uzsoki Teaching Hospital (Budapest, Hungary) were recruited into the study. Samples for research purposes were collected during surgery concomitantly with tissue samples taken for histopathological examination. The research project did not modify the treatment protocol of patients in any way. Tissue samples were stored in liquid nitrogen until further processing. The delay between the biopsy and immersion of the samples into liquid nitrogen was less than 30 min. The 4-μm

sections were cut with a cryostat and tissue slices were stored at –70C until staining. ErbB2 overexpression was established during the normal histopathological evaluation of the paraffin-embedded tumor samples at the Department of Pathology of the Uzsoki Teaching Hospital by immunohistochemistry using the 4B5 rabbit anti-ErbB2 monoclonal antibody (Ventana Medical Systems; Tucson, AZ) (van der Vegt et al. 2009). ErbB2 amplification was analyzed by fluorescence in situ hybridization using the Oncor INFORM system (Ventana Medical Systems) at the 2nd Department of Pathology, Semmelweis University, Budapest, as described previously (Lőrincz et al. 2006). Only patients showing strong positivity (2+ or 3+) in both tests were involved in the project. Patient follow-up data were collected after surgery by regular outpatient visits. The samples of 45 patients were stained. On average, ~15 images were taken and analyzed from every patient. The median age of patients was 68 years (5th and 95th percentiles were 36 and 87 years, respectively). The median weight of patients was 66 kg (5th and 95th percentiles were 46 and 85, respectively). The median height of patients was 161 cm (5th and 95th percentiles were 150 and 174, respectively). Seven of the 45 women admitted smoking. Eight of the 45 patients received neoadjuvant chemotherapy (cyclophosphamide + doxorubicin + 5-fluorouracil or docetaxel). The postsurgical treatment, which most patients received, is irrelevant for this study because samples were collected during surgery. The project was approved by the Science and Research Ethics Committee of the National Health Science Council (ad.335/PI/2007). Informed consent was obtained from all patients by the physicians responsible for their treatment.

Staining and Confocal Microscopy

Tissue sections were fixed in 4% formaldehyde followed by a two-step blocking procedure. First, sections were incubated in 1 mg/ml bovine serum albumin (BSA) to reduce nonspecific binding of antibodies followed by unlabeled avidin and biotin (components A and B of the endogenous biotin blocking kit, respectively; Invitrogen, Carlsbad, CA) to inhibit nonspecific attachment of fluorescent streptavidin to cellular, primarily mitochondrial, biotin. Then, samples were incubated in the presence of 5 µg/ml OP15 mAb against an intracellular epitope of ErbB2 (Calbiochem-Merck Biosciences; Schwalbach, Germany), Alexa Fluor 546–trastuzumab and 5 µg/ml biotinylated HABC (hyaluronic acid binding complex; isolated from the hyaluronan binding region of cartilage proteoglycan) overnight (Tammi et al. 1988). Trastuzumab was purchased from Roche (Basel, Switzerland) and labeled with Alexa Fluor 546 or Alexa Fluor 647 (Invitrogen) according to the instructions of the manufacturer. Afterwards, sections were labeled with

Alexa Fluor 488–streptavidin (Invitrogen) and Alexa Fluor 647 goat anti-mouse IgG (Invitrogen) for 60 min. Some sections were treated with hyaluronidase prior to staining. Digestion was carried out in the presence of 20 TRU/ml *Streptomyces* hyaluronidase (H1136; Sigma-Aldrich, St. Louis, MO) dissolved in PBS containing protease inhibitors (Complete Mini, Roche) at 37C overnight.

Image acquisition was carried out on an Olympus FV1000 confocal microscope (Olympus; Center Valley, PA) using a 60× oil immersion objective (NA = 1.35). Alexa Fluor 488, Alexa Fluor 546, and Alexa Fluor 647 were excited by the laser lines at 488 nm, 543 nm, and 633 nm, respectively. Fluorescence emissions of the three dyes were collected in the spectral regions of 515 ± 15 nm, 590 ± 35 nm, and 705 ± 50 nm, ensuring minimal spectral crosstalk. Due to day-to-day variations in the sensitivity and settings of the microscope, intensity corrections had to be carried out so that the images acquired on different days were comparable. Images of Rainbow calibration particles (BD Biosciences; Franklin Lakes, NJ) were captured every day, and their fluorescence intensities were normalized to each other, yielding correction factors that were applied to confocal images of tissue sections.

Image Analysis and Statistical Evaluation

Image analysis was carried out using a custom-written MATLAB program (Mathworks, Inc.; Natick, MA) implementing functions of the DipImage toolbox (Delft University of Technology, Delft, the Netherlands). Briefly, intensity trends (low-frequency background) were removed by top-hat filtering followed by segmentation of the image into membrane and non-membrane pixels. k-means clustering, region growing, and manually seeded watershed segmentation were used variably for segmentation, and the algorithm yielding the best result was chosen by visual inspection (Gonzalez et al. 2004). The average fluorescence intensity of a region without cells and connective tissue fibers was calculated, and this value was used for constant background subtraction. The mean fluorescence intensity of HABC (hyaluronan density) and the average of the pixelwise ratio of trastuzumab to OP15 intensities were calculated with the OP15 intensity representing the expression level of ErbB2. These parameters were averaged for each individual patient, and the trastuzumab/ErbB2 ratio was plotted against the HABC intensity, with each point representing a single patient. The strength of the linear correlation was determined by calculating the Pearson correlation coefficient. Samples were divided into three groups based on hyaluronan density (low, medium, and high), and their trastuzumab/OP15 ratios were compared using ANOVA followed by Tukey's honestly significant difference (HSD) test. Statistical calculations were carried out in SPSS 19 (SPSS, Inc., an IBM Company, Chicago, IL).
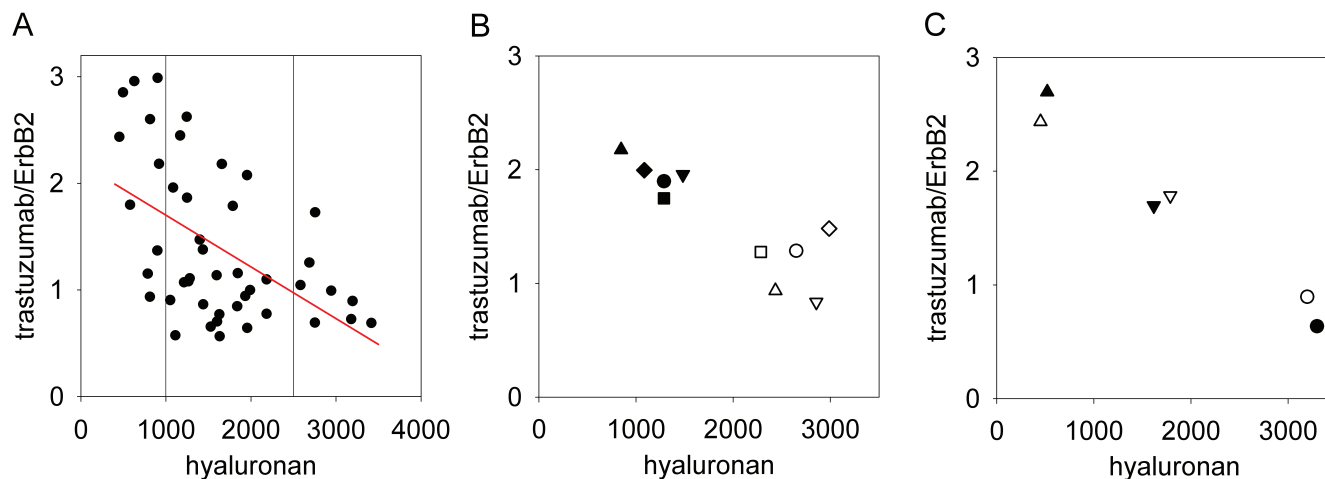
Figure 1. High hyaluronan density in tissue samples predicts low binding of trastuzumab. (A) Tissue samples were stained with trastuzumab (directly labeled with Alexa Fluor 546) and with an anti-ErbB2 antibody (OP15, indirectly labeled with Alexa Fluor 647–goat anti-mouse IgG) binding to an epitope in the intracellular domain of ErbB2, and hyaluronan was labeled with hyaluronic acid binding complex (HABC; indirectly stained with Alexa Fluor 488–streptavidin). The hyaluronan density and the trastuzumab/ErbB2 intensity ratio were calculated in the membrane mask (see Fig. 2). These parameters were averaged for each patient; therefore, every point in the graph represents the mean value of a single patient. The red line was fitted to the data points by linear regression ($r = -0.52$). The vertical reference lines show how the data set was divided into three groups (low, medium, and high hyaluronan density) for further statistical analysis. (B) Five patients whose samples displayed high hyaluronan content were chosen to demonstrate the effect of hyaluronidase treatment. Six sections from each of the selected patients were analyzed. Half of the samples from each patient were digested with hyaluronidase (filled symbols), whereas the rest of them were left untreated (open symbols). Sections were labeled in the same way as in part A, and the trastuzumab/ErbB2 ratio and the hyaluronan content were averaged for every patient. Identical shapes of the open and filled symbols correspond to the same patients. The increase in the normalized binding of trastuzumab was found to be significant using Student's paired *t*-test ($p<0.01$). (C) Three tissue samples were selected representing low, medium, and high hyaluronan density, and they were labeled as described in the legend to part A, but the fluorescent dyes for trastuzumab and OP15 were reversed—that is, trastuzumab directly labeled with Alexa Fluor 647 and OP15 indirectly labeled with Alexa Fluor 546–goat anti-mouse IgG (filled symbols, reverse labeling). Open symbols represent the results of the labeling procedure of the same three samples as described in part A ("forward" labeling). Fluorescence intensities of the HABC, trastuzumab, and OP15 images measured in the reverse-labeled samples were normalized to the corresponding fluorescence intensities of the forward-labeled samples. Identical shapes of the open and filled symbols correspond to the same samples labeled according to the two different labeling protocols.

Results

Trastuzumab binding is inhibited in patients with high hyaluronan production. We developed a method for the quantitative determination of the binding of trastuzumab normalized to ErbB2 expression in human breast cancer tissue samples. Sections were triple-stained for ErbB2 and hyaluronan expressions and with trastuzumab. Hyaluronan expression was measured by HABC staining, whereas a monoclonal antibody recognizing an intracellular epitope of ErbB2 was used to quantitate ErbB2 levels (mAb OP15). Cell membranes were identified, and the intensity of trastuzumab normalized to ErbB2 expression on a pixel-by-pixel basis was calculated in the cell membrane. The pericellular density of hyaluronan was also determined in the membrane mask, and the average ErbB2-normalized trastuzumab binding (i.e., mean of pixelwise trastuzumab/OP15 ratio) was plotted as a function of the mean pericellular hyaluronan density. The means were determined for every patient based on ~4 sections with ~4 images taken from every tissue

section (Figs. 1A, 2). Normalized trastuzumab binding showed a remarkable negative correlation with pericellular hyaluronan density, with a correlation coefficient of –0.52 (95% confidence interval was between –0.88 and –0.27, determined using Fisher's *Z* transform of the correlation coefficient). The square of the correlation coefficient was 0.27, implying that approximately one-quarter of the variance of normalized trastuzumab binding is accountable by pericellular hyaluronan density, assuming a linear relationship (Myers et al. 2010). The samples were divided into three groups (low, medium, and high hyaluronan density) based on the vertical reference lines in Figure 1A. Analysis of variance showed significant differences in the normalized trastuzumab binding of the three groups ($p<0.001$, Table 1). The mean normalized trastuzumab binding was more than two times higher in samples with low hyaluronan content than in those showing high hyaluronan density. Tukey's HSD test confirmed that the normalized trastuzumab binding in the medium and high hyaluronan groups was significantly different from that in the low hyaluronan
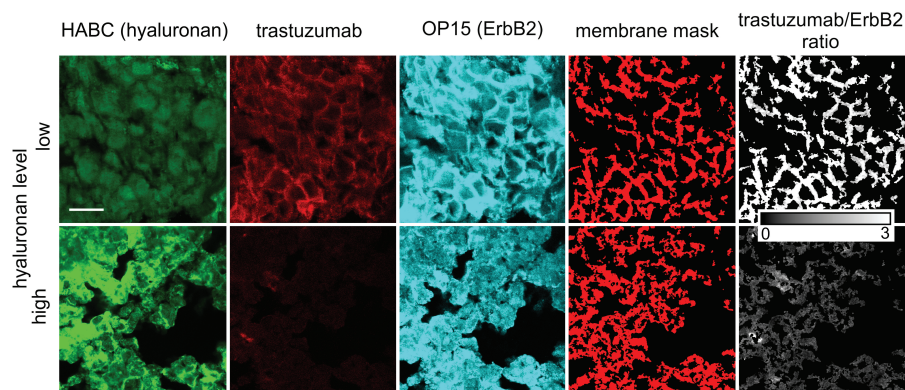
Figure 2. Representative images showing the anticorrelation between hyaluronan density and trastuzumab binding. Tissue samples were labeled with trastuzumab, OP15, and hyaluronic acid binding complex (HABC). MAb OP15 binds to an intracellular epitope on ErbB2, whereas HABC labels hyaluronan. Pixels corresponding to the membrane were identified as described in Materials and Methods. The background-corrected fluorescence intensities in the trastuzumab and OP15 images were divided by each other on a pixel-by-pixel basis, yielding the trastuzumab/ErbB2 image. The scale bar, valid for every image, is 20 μm.

samples (p=0.001). The effect size (the variability of the normalized trastuzumab binding compared with the measurement error), estimated by Cohen's f, was found to be 0.61 (Myers et al. 2010). These data present strong evidence for pericellular hyaluronan inhibiting the binding of trastuzumab to ErbB2.

Hyaluronidase digestion unmasks the trastuzumab binding epitope of ErbB2. To present independent evidence for the masking effect of hyaluronan, tissue sections were treated with hyaluronidase, and their hyaluronan content and normalized trastuzumab binding were compared with their untreated counterparts. The intensity of HABC staining was significantly decreased in samples treated with hyaluronidase. Decreased pericellular density of hyaluronan markedly enhanced the normalized binding of trastuzumab, implying that hyaluronidase efficiently unmasks the trastuzumab binding epitope of ErbB2 (Figs. 1B, 3).

Fluorescence resonance energy transfer (FRET) does not artificially introduce the negative correlation between trastuzumab binding and pericellular hyaluronan density. Several factors could generate the impression of a negative correlation between the binding of two fluorescent probes. FRET-induced quenching of Alexa Fluor 488–tagged HABC by Alexa Fluor 546–trastuzumab would lead to low HABC fluorescence intensity in pixels with high trastuzumab binding. Alternatively, quenching of the fluorescence of Alexa Fluor 546–trastuzumab by OP15 labeled by Alexa Fluor 647 would also lead to an artifactual decrease in the trastuzumab/OP15 fluorescence intensity ratio. If any of the above factors would have any effect in the generation of the observed negative correlation between normalized trastuzumab binding and pericellular hyaluronan density, then swapping of the fluorescent labels of trastuzumab and OP15 antibodies would change the correlation. Therefore, we

Table 1. Normalized Trastuzumab Binding Is Significantly Influenced by Pericellular Hyaluronan Density

Hyaluronan Density[a]	Normalized Trastuzumab Binding[b]	p Value[c]
Low (730 ± 175)	2.13 ± 0.77	NA
Medium (1565 ± 340)	1.25 ± 0.59	0.001
High (2940 ± 295)	1 ± 0.35	0.001

[a]Samples were divided into three groups based on their hyaluronan content according to the vertical reference lines in Figure 1A. Numbers represent the mean ± SD.
[b]Normalized trastuzumab binding was calculated by taking the average of the pixelwise trastuzumab/OP15 intensity ratios. The numbers represent the mean ± SD.
[c]p values of Tukey's honestly significant difference test comparing the trastuzumab binding of the medium and high hyaluronan groups to that of the low hyaluronan group. NA, not applicable.

selected one sample from each of the low, medium, and high hyaluronan groups and compared their trastuzumab/ErbB2 ratios when labeled with Alexa Fluor 546–trastuzumab and Alexa Fluor 647–OP15 ("forward" labeling) and when labeled with Alexa Fluor 546–OP15 and Alexa Fluor 647–trastuzumab ("reverse" labeling). We did not observe any significant difference in the tendency of the trastuzumab/ErbB2 ratio between the two labeling conditions (Fig. 1C). In addition, we have analyzed FRET between Alexa Fluor 546–trastuzumab and Alexa Fluor 647–labeled OP15 in cultured SKBR-3 breast cancer cells by flow cytometry. The almost complete absence of FRET between these two epitopes is in accordance with the large distance between the two antibodies due to their binding to opposite
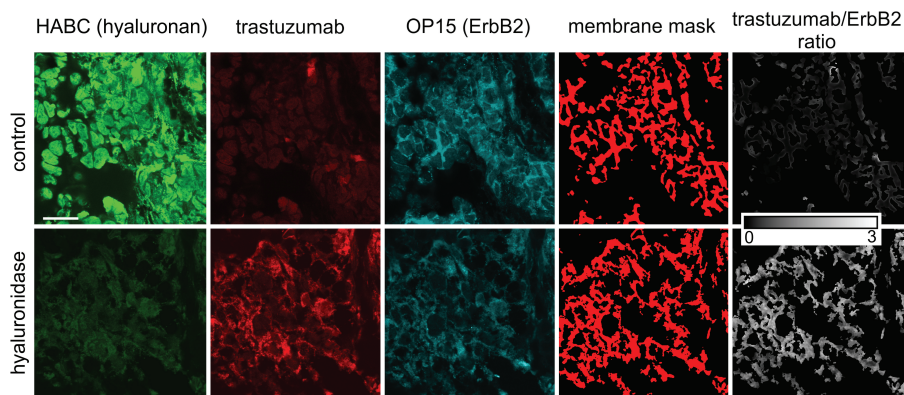
HABC (hyaluronan)   trastuzumab   OP15 (ErbB2)   membrane mask   trastuzumab/ErbB2 ratio

Figure 3. Representative images showing the effect of hyaluronidase treatment on the binding of trastuzumab. A tissue section was treated with hyaluronidase, whereas another sample from the same patient served as a control. Afterward, tissue samples were labeled and images were processed as described in Materials and Methods. The scale bar, valid for every image, is 20 μm.
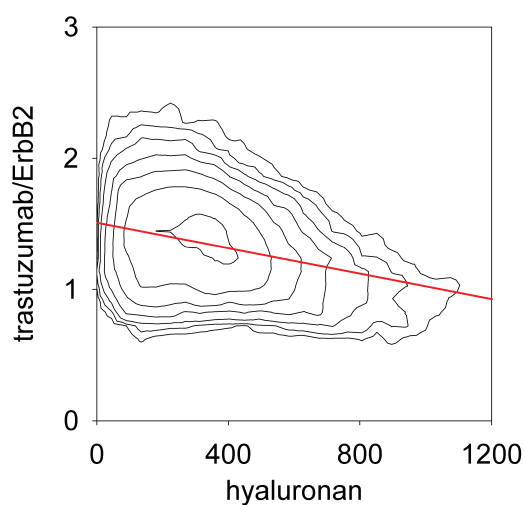

Figure 4. Anticorrelation between hyaluronan density and trastuzumab binding in a single confocal image. A tissue specimen was stained with trastuzumab, OP15 (for ErbB2), and hyaluronic acid binding complex (HABC). The trastuzumab/ErbB2 ratio and the hyaluronan density were evaluated in the membrane mask as described in Materials and Methods and they are displayed in a contour plot. The red line represents the linear regression of the trastuzumab/ErbB2 ratio on hyaluronan density ($r = -0.3$).

domains (intracellular vs. extracellular) of ErbB2 (Suppl. Fig. S1) and argues against an influence of FRET on normalized trastuzumab binding. We have also excluded that spectral cross-talk could lead to the observed negative correlation between trastuzumab binding and hyaluronan density because spectral bleed-through was negligible between the fluorescence channels. Therefore, we conclude that the observed negative correlation between fluorescence intensities reflects the negative correlation between the binding of the fluorescent probes.

The negative correlation between trastuzumab binding and hyaluronan density is typically present within a single specimen. The aforementioned observation of low binding of trastuzumab in the presence of a high local density of pericellular

hyaluronan was made when comparing samples from different patients. We also analyzed the same correlation within single specimens by inspecting the two-dimensional histograms (contour plots) of normalized trastuzumab binding versus hyaluronan density. The negative correlation between trastuzumab binding and pericellular hyaluronan concentration was present in ~2/3 of the samples (a typical example is shown in Fig. 4). The effect size was significantly lower (Cohen's $f = 0.31$) in this case than in the patientwise dataset in accordance with the lower correlation coefficient ($r = -0.3$) and with the less than 1.5-fold difference between the normalized mean trastuzumab binding in pixels with the lowest and highest hyaluronan densities. The pixelwise data, however, confirm that pericellular hyaluronan inhibits the binding of trastuzumab to ErbB2.

Discussion

Successful trastuzumab therapy hinges upon the binding of the antibody to its epitope on ErbB2. Although many factors, including the pharmacokinetics of the drug, influence the saturation of available trastuzumab binding sites, the accessibility of the membrane of ErbB2-overexpressing cells is an indispensable prerequisite for the antibody to exert its effects. In the current article, we show that pericellular hyaluronan expression inhibits trastuzumab binding in ErbB2-overexpressing human breast cancer samples. The demonstration of the anticorrelation between hyaluronan density and normalized trastuzumab binding was made possible by (1) limiting the evaluation of pixel intensities to the cell membrane and (2) quantitative image analysis normalizing the binding of trastuzumab to the expression level of ErbB2, which eliminated the large intratumor variation of trastuzumab binding due to different ErbB2 expression levels. It follows from the method that pericellular density of hyaluronan, and not the total hyaluronan content, was determined and correlated with normalized trastuzumab binding. The fact that our method captures the density of pericellular hyaluronan is important because pericellular

hyaluronan has been shown to create an "exclusion zone" around cells whose diameter must depend on the size of the probe with which it is determined (Rilla et al. 2008). The current findings are in agreement with our previous results in which hyaluronan-mediated inhibition of trastuzumab binding was demonstrated in vitro and in mouse xenograft experiments (Pályi-Krekk et al. 2007). The reliability of the establishment of a negative correlation is dependent on the determination of ErbB2 expression levels in the cell membrane. As we have previously shown, the OP15 antibody is insensitive to masking, and its fluorescence intensity reports the expression level of ErbB2 (Nagy et al. 2005). We have also excluded that spectral crosstalk or FRET could have led to the observed anticorrelation.

The mechanism of how hyaluronan inhibits trastuzumab binding is unknown, although there are a number of plausible assumptions. (1) It is possible that the dense hyaluronan meshwork directly covers or masks the trastuzumab binding epitope of ErbB2 (Toole 2004; Rilla et al. 2008). (2) Alternatively, hyaluronan has been implicated as one of the factors leading to increased interstitial pressure in malignant tumors, which results in blood vessel collapse and inhibition of pressure difference–driven transport of drug molecules to the center of the tumor (Jain 1988; Fukumura and Jain 2007). (3) In addition, diffusion may also be slowed down by hyaluronan or other components of the extracellular matrix (Lieleg and Ribbeck 2011). The validity of the first explanation is substantiated by two of our previous findings. (a) We have shown that overproduction of hyaluronan inhibits trastuzumab binding in vitro, where explanations 2 and 3 are irrelevant or can be considered of less importance (Pályi-Krekk et al. 2007). (b) We have demonstrated that overexpression of another molecule, MUC4, can also lead to epitope masking in vitro (Nagy et al. 2005). With regard to MUC4-dependent masking, we have shown that the phenomenon is not universal because the binding of the anti-ErbB2 antibody 2C4 (original mouse version of pertuzumab), whose epitope is known to be located far from the plasma membrane (Nagy et al. 1998; Franklin et al. 2004), was not inhibited, whereas the trastuzumab-binding epitope, known to be close to the membrane (Nagy et al. 1998; Cho et al. 2003), was significantly masked. Therefore, we believe that the proximity of an epitope to the membrane is an important factor in determining the efficiency of masking. Independent of the mechanism of the masking effect shown in the current article, the demonstration that hyaluronan depletion results in improved tumor penetration of conventional chemotherapeutic drugs, liposomes, and trastuzumab in animal models argues in favor of hyaluronan being an important factor limiting the accessibility of drug binding sites in cancer (Pályi-Krekk et al. 2007; Thompson et al. 2010). In addition, hyaluronan can also block the migration of immunocompetent cells to trastuzumab on ErbB2-expressing cancer cells and thereby interfere with the immune system–mediated effects of the antibody.

The correlation coefficient between pericellular hyaluronan density and normalized trastuzumab binding was found to be –0.52. Although this value of the correlation coefficient is significantly different from zero, it can be considered to indicate a medium-strong relation between the two variables (Myers et al. 2010). In addition, the inhibitory effect of hyaluronan on trastuzumab binding was also demonstrated by the fact that hyaluronidase treatment unmasked the trastuzumab binding epitope of ErbB2. However, it must be noted that trastuzumab binding is expected to be influenced by a multitude of factors. Therefore, the correlation coefficient of the bivariate regression of normalized trastuzumab binding on hyaluronan expression will be lower than the ideal strength of the relationship between the two variables, which could be observed if the confounding variables would not have any effect at all (Myers et al. 2010). The correlation coefficient between normalized trastuzumab binding and pericellular hyaluronan density determined on a single specimen was lower than the global correlation coefficient calculated on patientwise data. The correlation coefficient is the product of the slope of the regression line and the ratio between the standard deviations (SD) of the predictor and predicted variables (Myers et al. 2010). Because the slopes of the two regression lines were identical within experimental error, the smaller correlation coefficient in a single specimen is the consequence of the decreased ratio of $SD_{predictor}/SD_{predicted}$ (predictor and predicted variables are the pericellular hyaluronan density and normalized trastuzumab binding, respectively), which may be caused by the relatively large $SD_{predicted}$ in single specimens due to intratumor heterogeneity and measurement error. The effect of these factors is made smaller in patientwise data because they are averaged, yielding a more reliable prediction characterized by a larger correlation coefficient. Overproduction of hyaluronan has already been shown to lead to poor prognosis in breast cancer (Auvinen et al. 2000; Wernicke et al. 2003). Therefore, any possible correlation between hyaluronan-induced inhibited binding of trastuzumab with the survival of breast cancer patients is expected to be confounded by other effects of hyaluronan on the clinical outcome.

In summary, we present evidence that hyaluronan inhibits trastuzumab binding to ErbB2-overexpressing breast cancer cells in human tissue samples. This anticorrelation identifies another effect of hyaluronan in promoting cancer progression and resistance to chemotherapy and immunotherapy. Our data call for testing the hyaluronan level of ErbB2-overexpressing tissue samples and warrant further development of drug candidates that lower tissue hyaluronan levels.

Acknowledgements

Declaration of Conflicting Interests

Funding

References

Auvinen P, Tammi R, Parkkinen J, Tammi M, Agren U, Johansson R, Hirvikoski P, Eskelinen M, Kosma VM. 2000. Hyaluronan in peritumoral stroma and malignant cells associates with breast cancer spreading and predicts survival. Am J Pathol. 156:529–536.

Barok M, Isola J, Pályi-Krekk Z, Nagy P, Juhász I, Vereb G, Kauraniemi P, Kapanen A, Tanner M, Szöllősi J. 2007. Trastuzumab causes antibody-dependent cellular cytotoxicity-mediated growth inhibition of submacroscopic JIMT-1 breast cancer xenografts despite intrinsic drug resistance. Mol Cancer Ther. 6:2065–2072.

Bourguignon LY, Peyrollier K, Gilad E, Brightman A. 2007. Hyaluronan-CD44 interaction with neural Wiskott-Aldrich syndrome protein (N-WASP) promotes actin polymerization and ErbB2 activation leading to β-catenin nuclear translocation, transcriptional up-regulation, and cell migration in ovarian tumor cells. J Biol Chem. 282:1265–1280.

Cho HS, Mason K, Ramyar KX, Stanley AM, Gabelli SB, Denney DW Jr, Leahy DJ. 2003. Structure of the extracellular region of HER2 alone and in complex with the Herceptin Fab. Nature. 421:756–760.

Clynes RA, Towers TL, Presta LG, Ravetch JV. 2000. Inhibitory Fc receptors modulate in vivo cytoxicity against tumor targets. Nat Med. 6:443–446.

Day AJ, Prestwich GD. 2002. Hyaluronan-binding proteins: tying up the giant. J Biol Chem. 277:4585–4588.

Di Cosimo S, Baselga J. 2008. Targeted therapies in breast cancer: where are we now? Eur J Cancer. 44:2781–2790.

Di Cosimo S, Baselga J. 2010. Management of breast cancer with targeted agents: importance of heterogeneity. Nat Rev Clin Oncol. 7:139–147.

Franklin MC, Carey KD, Vajdos FF, Leahy DJ, de Vos AM, Sliwkowski MX. 2004. Insights into ErbB signaling from the structure of the ErbB2-pertuzumab complex. Cancer Cell. 5:317–328.

Fukumura D, Jain RK. 2007. Tumor microenvironment abnormalities: causes, consequences, and strategies to normalize. J Cell Biochem. 101:937–949.

Gonzalez RC, Woods RE, Eddins SL. 2004. Image segmentation. In: Gonzalez RC, Woods RE, Eddins SL, editors. Digital image processing using Matlab. Upper Saddle River, NJ: Pearson Prentice Hall. p. 378–425.

Hynes NE, MacDonald G. 2009. ErbB receptors and signaling pathways in cancer. Curr Opin Cell Biol. 21:177–184.

Itano N, Kimata K. 2008. Altered hyaluronan biosynthesis in cancer progression. Semin Cancer Biol. 18:268–274.

Izumi Y, Xu L, di Tomaso E, Fukumura D, Jain RK. 2002. Tumour biology: herceptin acts as an anti-angiogenic cocktail. Nature. 416:279–280.

Jain RK. 1988. Determinants of tumor blood flow: a review. Cancer Res. 48:2641–2658.

Junttila TT, Akita RW, Parsons K, Fields C, Lewis Phillips GD, Friedman LS, Sampath D, Sliwkowski MX. 2009. Ligand-independent HER2/HER3/PI3K complex is disrupted by trastuzumab and is effectively inhibited by the PI3K inhibitor GDC-0941. Cancer Cell. 15:429–440.

Lane HA, Motoyama AB, Beuvink I, Hynes NE. 2001. Modulation of p27/Cdk2 complex formation through 4D5-mediated inhibition of HER2 receptor signaling. Ann Oncol. 12(Suppl 1):S21–S22.

Lieleg O, Ribbeck K. 2011. Biological hydrogels as selective diffusion barriers. Trends Cell Biol. 21:543–551.

Lower EE, Glass E, Blau R, Harman S. 2009. HER-2/neu expression in primary and metastatic breast cancer. Breast Cancer Res Treat. 113:301–306.

Lőrincz T, Tóth J, Badalian G, Tímár J, Szendrői M. 2006. HER-2/neu genotype of breast cancer may change in bone metastasis. Pathol Oncol Res. 12:149–152.

Misra S, Ghatak S, Toole BP. 2005. Regulation of MDR1 expression and drug resistance by a positive feedback loop involving hyaluronan, phosphoinositide 3-kinase, and ErbB2. J Biol Chem. 280:20310–20315.

Molina MA, Codony-Servat J, Albanell J, Rojo F, Arribas J, Baselga J. 2001. Trastuzumab (herceptin), a humanized anti-Her2 receptor monoclonal antibody, inhibits basal and activated Her2 ectodomain cleavage in breast cancer cells. Cancer Res. 61:4744–4749.

Mukohara T. 2011. Mechanisms of resistance to anti-human epidermal growth factor receptor 2 agents in breast cancer. Cancer Sci. 102:1–8.

Myers JL, Well AD, Lorch RF. 2010. Research design and statistical analysis. 3rd ed. New York: Routledge.

Nagata Y, Lan KH, Zhou X, Tan M, Esteva FJ, Sahin AA, Klos KS, Li P, Monia BP, Nguyen NT, et al. 2004. PTEN activation contributes to tumor inhibition by trastuzumab, and loss of PTEN predicts trastuzumab resistance in patients. Cancer Cell. 6:117–127.

Nagy P, Bene L, Balázs M, Hyun WC, Lockett SJ, Chiang NY, Waldman F, Feuerstein BG, Damjanovich S, Szöllősi J. 1998. EGF-induced redistribution of erbB2 on breast tumor cells: flow and image cytometric energy transfer measurements. Cytometry. 32:120–131.

Nagy P, Friedländer E, Tanner M, Kapanen AI, Carraway KL, Isola J, Jovin TM. 2005. Decreased accessibility and lack of activation of ErbB2 in JIMT-1, a herceptin-resistant, MUC4-expressing breast cancer cell line. Cancer Res. 65:473–482.

Nahta R, Esteva FJ. 2006. Herceptin: mechanisms of action and resistance. Cancer Lett. 232:123–138.

Pályi-Krekk Z, Barok M, Isola J, Tammi M, Szöllősi J, Nagy P. 2007. Hyaluronan-induced masking of ErbB2 and CD44-enhanced trastuzumab internalisation in trastuzumab resistant breast cancer. Eur J Cancer. 43:2423–2433.

Pályi-Krekk Z, Barok M, Kovács T, Saya H, Nagano O, Szöllősi J, Nagy P. 2008. EGFR and ErbB2 are functionally coupled to CD44 and regulate shedding, internalization and motogenic effect of CD44. Cancer Lett. 263:231–242.

Pentassuglia L, Sawyer DB. 2009. The role of Neuregulin-1beta/ErbB signaling in the heart. Exp Cell Res. 315:627–637.

Rilla K, Tiihonen R, Kultti A, Tammi M, Tammi R. 2008. Pericellular hyaluronan coat visualized in live cells with a fluorescent probe is scaffolded by plasma membrane protrusions. J Histochem Cytochem. 56:901–910.

Ross JS, Fletcher JA, Linette GP, Stec J, Clark E, Ayers M, Symmans WF, Pusztai L, Bloom KJ. 2003. The Her-2/neu gene and protein in breast cancer 2003: biomarker and target of therapy. Oncologist. 8:307–325.

Sironen RK, Tammi M, Tammi R, Auvinen PK, Anttila M, Kosma VM. 2011. Hyaluronan in human malignancies. Exp Cell Res. 317:383–391.

Smith I, Procter M, Gelber RD, Guillaume S, Feyereislova A, Dowsett M, Goldhirsch A, Untch M, Mariani G, Baselga J, et al. 2007. 2-year follow-up of trastuzumab after adjuvant chemotherapy in HER2-positive breast cancer: a randomised controlled trial. Lancet. 369:29–36.

Sperinde J, Jin X, Banerjee J, Penuel E, Saha A, Diedrich G, Huang W, Leitzel K, Weidler J, Ali SM, et al. 2010. Quantitation of p95HER2 in paraffin sections by using a p95-specific antibody and correlation with outcome in a cohort of trastuzumab-treated breast cancer patients. Clin Cancer Res. 16:4226–4235.

Storr SJ, Woolston CM, Barros FF, Green AR, Shehata M, Chan SY, Ellis IO, Martin SG. 2011. Calpain-1 expression is associated with relapse-free survival in breast cancer patients treated with trastuzumab following adjuvant chemotherapy. Int J Cancer. 129:1773–1780.

Takahashi Y, Li L, Kamiryo M, Asteriou T, Moustakas A, Yamashita H, Heldin P. 2005. Hyaluronan fragments induce endothelial cell differentiation in a CD44- and CXCL1/GR01-dependent manner. J Biol Chem. 280:24195–24204.

Tammi R, Ripellino JA, Margolis RU, Tammi M. 1988. Localization of epidermal hyaluronic acid using the hyaluronate binding region of cartilage proteoglycan as a specific probe. J Invest Dermatol. 90:412–414.

Thompson CB, Shepard HM, O'Connor PM, Kadhim S, Jiang P, Osgood RJ, Bookbinder LH, Li X, Sugarman BJ, Connor RJ, et al. 2010. Enzymatic depletion of tumor hyaluronan induces antitumor responses in preclinical animal models. Mol Cancer Ther. 9:3052–3064.

Toole BP. 2004. Hyaluronan: from extracellular glue to pericellular cue. Nat Rev Cancer. 4:528–539.

Toole BP, Wight TN, Tammi MI. 2002. Hyaluronan-cell interactions in cancer and vascular disease. J Biol Chem. 277:4593–4596.

Toole BP, Zoltan-Jones A, Misra S, Ghatak S. 2005. Hyaluronan: a critical component of epithelial-mesenchymal and epithelial-carcinoma transitions. Cells Tissues Organs. 179:66–72.

Twarock S, Freudenberger T, Poscher E, Dai G, Jannasch K, Dullin C, Alves F, Prenzel K, Knoefel WT, Stoecklein NH, et al. 2011. Inhibition of oesophageal squamous cell carcinoma progression by in vivo targeting of hyaluronan synthesis. Mol Cancer. 10:30.

Udabage L, Brownlee GR, Waltham M, Blick T, Walker EC, Heldin P, Nilsson SK, Thompson EW, Brown TJ. 2005. Antisense-mediated suppression of hyaluronan synthase 2 inhibits the tumorigenesis and progression of breast cancer. Cancer Res. 65:6139–6150.

Urakawa H, Nishida Y, Wasa J, Arai E, Zhuo L, Kimata K, Kozawa E, Futamura N, Ishiguro N. 2012. Inhibition of hyaluronan synthesis in breast cancer cells by 4-methylumbelliferone suppresses tumorigenicity in vitro and metastatic lesions of bone in vivo. Int J Cancer. 130:454–466.

van der Vegt B, de Bock GH, Bart J, Zwartjes NG, Wesseling J. 2009. Validation of the 4B5 rabbit monoclonal antibody in determining Her2/neu status in breast cancer. Mod Pathol. 22:879–886.

Weigel PH, DeAngelis PL. 2007. Hyaluronan synthases: a decade-plus of novel glycosyltransferases. J Biol Chem. 282:36777–36781.

Weinstein IB, Joe A. 2008. Oncogene addiction. Cancer Res. 68:3077–3080.

Wernicke M, Pineiro LC, Caramutti D, Dorn VG, Raffo MM, Guixa HG, Telenta M, Morandi AA. 2003. Breast cancer stromal myxoid changes are associated with tumor invasion and metastasis: a central role for hyaluronan. Mod Pathol. 16:99–107.